RSC Advances

PAPER

View Article Online
View Journal | View Issue

Check for updates

Cite this: *RSC Adv.*, 2017, **7**, 27522

Tailor-made zwitterionic polyurethane coatings: microstructure, mechanical property and their antimicrobial performance

Chunhua Wang,[a] Chunfeng Ma,*[b] Changdao Mu[c] and Wei Lin *[a]

Antimicrobial coating is of great important in leather finishing. Herein, we report a newly synthesized polyurethane with zwitterionic sulfobetaine side groups and evaluate their performance in the antifouling leather coatings. The microstructure of the synthesized zwitterionic polyurethane (iNPU) films has been examined by Fourier transform infrared (FTIR), X-ray diffraction (XRD) and atomic force microscopy (AFM) in order to understand how it influences the mechanical and surface properties. Our results show that introduction of zwitterionic groups into polyurethane can markedly increase the degree of micro-phase separation between the hard and soft segments of the PU chains since the incorporated zwitterionic group leads to more hydrogen bonding and polar interactions, making the hard components to be more thermodynamically incompatible with the soft segments. As the content of the incorporated zwitterionic content increases, the ordered structure in PU chains is reduced, and the micro-phase separation degree is increased. Therefore, the tensile strength and elongation at break of the iNPU films are significantly improved. Dynamic mechanical thermal analysis (DMTA) results further indicate that the T_g of the iNPU coatings decreases, and the deformability greatly increases at a higher content of zwitterionic group. Water contact angle (WCA) measurements reveal the improved surface wetting property due to the presence of zwitterionic group. The antibacterial testing shows that the iNPU coated leather surfaces exhibit reasonably good anti-mold adhesion performance, although the iNPU films do not show apparent contact-killing antibacterial property against *E. coli* and *S. aureus*. The present zwitterionic polyurethane is thus can be potentially used as antimicrobial adhesive leather coating materials.

Received 19th April 2017
Accepted 17th May 2017

DOI: 10.1039/c7ra04379a

rsc.li/rsc-advances

Open Access Article. Published on 23 May 2017. Downloaded on 2/10/2026 8:12:29 PM.
This article is licensed under a Creative Commons Attribution 3.0 Unported Licence.

1 Introduction

Producing anti-biofouling coatings or membranes is of great interest in numerous technological applications such as water purification,[1] medical implants and devices,[2] marine anti-fouling,[3] food packaging,[4] textiles,[5] and leather finishing.[6] As far as the coatings for leather antifouling finishing are concerned, restrictions on the use of biocidal agents and high-risk chemicals potentially toxic to human beings have necessitated the development of environmental-friendly antimicrobial coatings. Polyurethane is one of the most favourable matrix polymers, biocompatible, biodegradable and versatile. Polyurethane coatings exhibit excellent mechanical properties, good hardness and high abrasion resistance resulting from rational content of hard segment and molecular weight of soft segment, *etc.* In leather industry, waterborne polyurethane is largely used as the finishing of crust leather to improve surface appearance and performances.[7]

For fabricating antifouling coatings, one of the major approaches is to create the surface that can prevent protein and microbes from attaching. Functionalization of surfaces with poly(ethylene glycol) (PEG) or oligo(ethylene glycol) has been widely investigated for imparting adhesion resistance in the past decades.[8,9] As a promising alternative to PEG-based coatings, incorporating of zwitterion groups onto polymer surfaces has also been designed for their reasonably good biocompatibility and protein resistance properties. It has been reported that polyurethanes containing zwitterionic phosphorylcholine (PC),[10] carboxybetaine (CB)[11] or sulfobetaine (SB)[12] moieties all showed significant and comparable reduction in the amount of protein adhesion. The most prominent hypothesis behind such activity is that the zwitterions with a balanced charge and minimized dipole bind strongly to water *via* electrostatic interactions, creating a hydration layer that does not allow proteins to adhere to the surface.[13] Recently, we have developed a novel approach to prepare antifouling polyurethane with varied length of zwitterionic SB as the side chains,[14] which can effectively resist nonspecific protein adsorption on underwater

[a]*Department of Biomass and Leather Engineering, Key Laboratory of Leather Chemistry and Engineering of Ministry of Education, Sichuan University, Chengdu, 610065, PR China. E-mail: wlin@scu.edu.cn*

[b]*Faculty of Material and Science and Engineering, South China University of Technology, Guangzhou, 510640, PR China. E-mail: msmcf@scut.edu.cn*

[c]*Department of Pharmaceutical and Bioengineering, School of Chemical Engineering, Sichuan University, Chengdu, 610065, PR China*

This journal is © The Royal Society of Chemistry 2017

Open Access Article. Published on 23 May 2017. Downloaded on 2/10/2026 8:12:29 PM.
This article is licensed under a Creative Commons Attribution 3.0 Unported Licence.

surfaces as measured by quartz crystal microbalance with dissipation technique (QCM-D). Nevertheless, simple protein resistance experiments do not truly represent the effectiveness against airborne microbes proposed by practical applications in surface finishing of macroscopic materials. So far, little information is available on the antimicrobial adhesion and antibacterial activity of zwitterionic polyurethane (iNPU) leather coatings.

In the present work, the tailor-made polyurethanes with well-defined short SB zwitterionic side chains or side groups are synthesized as our previous report.[15] Since the chain extender has considerable effect on the micro-phase separation of the polyurethanes, we focus on studying the effects of zwitterionic groups included in the chain extender on the microstructure and mechanical property using FTIT, XRD, AFM and DMTA. Furthermore, the iNPU finished leather surfaces have been tested for the anti-microbial adhesion against airborne *A. niger* spores to broaden the scope of iNPU applications as antifouling films. And the antibacterial property of the coating films is evaluated by agar diffusion method to further explore the antifouling mechanism. Our aim is to develop environmental-friendly polyurethane coatings with the ability of combating microbial contamination.

2 Experimental

2.1 Materials

Poly(tetramethylene oxide) (PTMG) (M_w = 2000 g mol^{-1}), 1,3-propane sultone (1,3-PS), 3-isocyanatomethyl-3,5,5-trimethylcyclohexyl isocyanate (IPDI), 3-mercapto-1,2-propanediol (TPG) and 2-(dimethylamino)ethyl methacrylate (DMAEMA) were purchased from Aladdin (Shanghai). 1,4-Butane diol (1,4-BD) and dibutyltin dilaurate (DBTDL) were purchased from Aldrich. PTMG, DMAEMA and 1,4-BD were purified under a reduced pressure before use. Tetrahydrofuran (THF) was refluxed over CaH_2 and distilled. *Staphylococcus aureus* (*S. aureus*, ATCC 25923), *Escherichia coli* (*E. coli*, ATCC 25922) and *Aspergillus niger* (*A. niger*, ATCC 9642) were obtained as indicators of experimental microbes. Other reagents were used as received without any pre-treatment.

2.2 Synthesis of zwitterionic polyurethane (iNPU)

The preparation of iNPU contains three main procedures: synthesis of chain extender DMA(OH)$_2$, preparation of polyurethane with DMAEMA side groups (NPU), and ionization or betainization of NPU to obtain the zwitterionic polyurethanes, as our previous report.[15] Briefly, photoinitiating thiol–ene click reaction between DMAEMA and TPG was utilized to synthesize dihydroxy-terminated DMAEMA (DMA(OH)$_2$) under UV catalysis in the presence of photoinitiator, 2,2-dimethoxy-2-phenyl acetophenone (DMPA). Then, DMA(OH)$_2$ is incorporated into polyurethane as a chain extender by reacting with the –NCO of the pre-polymer obtained from the reaction of IPDI with PTMG. Meanwhile, another chain extender 1,4-BD was simultaneously introduced for the synthesis of NPU. The NPU further reacted with 1,3-propane sultone to obtain iNPU. The feed molar ratio of PTMG/IPDI/chain extenders was 1 : 6.7 : 5.7. The weight percentage of DMA(OH)$_2$ was controlled by changing the molar ratio of DMA(OH)$_2$ and 1,4-BD. Then, the ionized polyurethane with different contents of DMAEMA side groups is designated as iNPU-*x*, where *x* is the weight percentage of DMA(OH)$_2$ calculated according to the molar ratio. In contrast, PU-0 without DMA(OH)$_2$ was also synthesized from IPDI, PTMG and 1,4-BD as reference. The content of hard components in polyurethane increased from ~50% for PU-0 to ~60% for iNPU-30 due to the higher M_w of DMA(OH)$_2$ (M_w = 265).

2.3 Formation of PU-0 and iNPU coating films

The solid contents of PU-0 and iNPU solutions in THF were adjusted to 20 wt%, respectively. The PU and iNPU coating films were formed *via* casting a designated mass of the polyurethane solution into polytetrafluoroethylene (PTFE) moulds followed by drying at 40 °C until constant weight. The films were stored in a desiccator at 25 °C and 50 ± 3% relative humidity before measurements.

2.4 Fourier transform infrared (FTIR) spectroscopy

FT-IR spectra of the samples were obtained on a Bruker VECTOR-22 IR spectrometer using the KBr disk method. Each sample was scanned for 64 times in the range of 400–4000 cm^{-1} with a spectral resolution of 4 cm^{-1}.

2.5 X-ray diffraction (XRD)

X-ray diffraction data were obtained using an 18 KW rotating anode X-ray diffractometer (MXPAHF, Japan) with a fixed Cu K radiation of 0.154 nm and a sample to detector distance of 10 cm. It allowed the wide angle diffraction feature of polyurethane to be observed at a resolution of 0.08 nm. The samples were scanned in the range of diffraction angle 2θ from 5° to 60° with a scanning rate of 2° min^{-1} at ambient temperature and humidity. The Peakfit4 (AISL software), one-dimensional peak fitting program, was used to determine the peak size shapes and the integrated intensity of the linear profiles. The real lattice space *d*, which represents characteristic structure dimension of polymer, can be calculated by $\lambda = 2d \sin\theta$, where λ is the X-ray wavelength and θ is half of the diffraction angle.[16]

2.6 Atomic force microscopy (AFM)

AFM was used to observe the topographic micro-phase separation of polyurethane. The PU-0 and iNPU films were set onto a freshly cleaved mica substrate, which were then placed in a desiccator for 48 h at room temperature before test. AFM was performed on a Shimadzu SPM-9600 equipped with Si cantilevers in a non-contact (taping) mode. For each sample, the analyses were made at three different points to confirm the consistency of the observed morphology.

2.7 Tensile testing

The stress–strain curves, tensile strength (TS) and elongation at break (EB) of polyurethane samples were evaluated with a servo control universal GT-AI-7000S Leather Tension Testing Machine

Open Access Article. Published on 23 May 2017. Downloaded on 2/10/2026 8:12:29 PM.
This article is licensed under a Creative Commons Attribution 3.0 Unported Licence.

(Gotech, Testing Machines Inc., China) using the standard testing method ASTM D882-97.[17] Two rectangular strips (width 5 mm, length 50 mm) were cut from each film to determine the mechanical property. Initial grip separation was set at 50 mm and stretching rate was at 100 mm min^{-1}. TS (MPa) was calculated from TS = F_{max}/A, in which F_{max} stands for the maximum load (N) needed to pull the sample apart, and A stands for cross-sectional area (m^2) of the samples. EB (%) was calculated by EB = $(L/25) \times 100$, in which L stands for the elongation of each film at rupture (mm), and 25 stand for the initial grip length (mm) of each sample. The testing was conducted twice for each sample.

2.8 Dynamic mechanical thermal analysis (DMTA)

A sinusoidal varying stress has been applied to the film samples in DMA measurement, producing an oscillating strain which lags behind the applied stress by a phase angle delta. The dynamic maximum force in the experiment was 2 N and the maximum amplitude was 20 μm. The thermomechanical analysis were performed on a dynamic mechanical analyzer (NETZSCH DMA242C, Germany) from −150 °C to 100 °C at a heating rate of 10 °C min^{-1} and a frequency of 0.1 Hz and 1 Hz under nitrogen atmosphere. The dynamic storage modulus E', dynamic loss modulus E'' and tan delta (tan delta = E''/E') as a function of temperature were obtained. All the samples were subjected to identical controlled temperature and controlled atmosphere.

2.9 Surface contact angle

The surface hydrophobicity and wettability of PU-0 and iNPU coating films were evaluated through the water contact angle (WCA) measurement. The sample with areas of 1 cm × 3 cm was fixed on smooth clean glass slide, and a 10 μL water droplet was dropped onto the sample. The static contact angle was texted using Automatic Surface Tension Determinator (Detaphysics, Germany). Five groups of data were recorded and the average values were gained.

2.10 Anti-microbe adhesion experiment of leather samples finished with PU-0 and iNPU

The antimicrobial adhesion property of the coatings were investigated by observing the absorption of molds on the surface of goatskin leather samples coated with PU-0 and iNPU respectively in a simulated storage environment. The leather samples were first fixed on a white plastic sheet with small nails. Then, the sheet was vertically positioned in a small incubator with a relative humidity of 90% and a constant temperature of 28 °C. And a culture plate of *A. niger* was also put in the enclosed environment to provide *A. niger* spores. With the time extending, the spore in the incubator may be absorbed onto the surface of leather samples and further grow and propagate, forming black colonies. The samples were observed and photographed at different incubation days.

2.11 Antibacterial test of polyurethane coating films

The antibacterial property of iNPU coatings was evaluated using Gram-negative bacterium *E. coli* and Gram-positive bacterium *S. aureus* as the test cultures by the method of Kirby–Bauer disk diffusion analysis (KBA), also known as agar diffusion method.[18] Test samples (2 cm in diameter) cut from the polyurethane films were sterilized through UV irradiation for 1 h before use. Overnight aged active bacteria (200 μL, 1 × 106 UF mL^{-1}) were inoculated in the nutrient agar plates. The sterilized polyurethane samples were placed onto the nutrient agar plates and then incubated at 37 °C.

3 Results and discussion

3.1 FT-IR analysis

Hydrogen bond is the most important interaction in polyurethanes and tends to influence the macro-property of the coatings.[19] The N–H band absorption and C=O band absorption of PU-0 and iNPU-30 are shown in Fig. 1a and b, respectively. Generally, the peak at 3289–3295 cm^{-1} is attributed to the bonded N–H with ether oxygen of the soft segment,[20] while 3300–3340 cm^{-1} is attributed to the bonded N–H with the carbonyl in the urethane.[21] The broader N–H band moving to higher wavenumber of iNPU-30 than that of PU-0 indicates more hydrogen bonded interactions within hard segments of iNPU-30, due to the introduction of the zwitterionic group. Besides, Fig. 1b shows the broad absorption of 1650–1730 cm^{-1} for both iNPU-30 and PU-0, indicating the co-existence of free C=O and hydrogen-bonded one. Meanwhile, a new peak observed at 1650 cm^{-1} in iNPU-30 is attributed to the stretching of the hydrogen-bonded carbonyl in allophanate,[22] which may

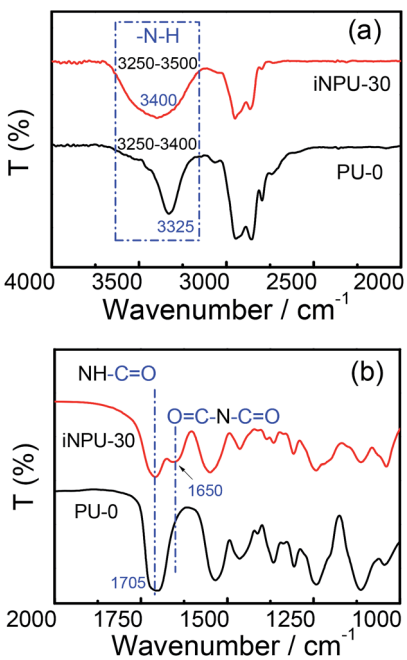

Fig. 1 FT-IR spectra of PU-0 and iNPU-30 ranging from (a) 2000–4000 cm^{-1}, and (b) 1000–2000 cm^{-1}.

This journal is © The Royal Society of Chemistry 2017

Open Access Article. Published on 23 May 2017. Downloaded on 2/10/2026 8:12:29 PM.
This article is licensed under a Creative Commons Attribution 3.0 Unported Licence.

be formed by the reaction of isocyanate groups with urethane[23] during the synthesis of iNPU. Thus, the hard components which consist of chain extenders, isocyanate and allophanate, become more thermodynamically incompatible with soft segment than simple urethane groups.

3.2 XRD analysis

The X-ray diffraction patterns of PTMG and the resulting polyurethanes are depicted in Fig. 2a and b, respectively. From Fig. 2a, two sharp and strong peaks appearing at $2\theta = 19.8°$ and 24.4° for PTMG polyol correspond to a *d*-spacing value of 0.45 nm and 0.36 nm respectively, calculated through the Bragg's equation $\lambda = 2d \sin \theta$, showing its crystalline characteristic.[24,25] In Fig. 2b, the broad peak around $2\theta = 20.4°$ for both PU and iNPU indicate the existence of amorphous structure of the polyurethanes. However, it cannot exclude the presence of small crystalline structures and partial ordered arrangement of PU chain segments.[26] It is noted that with the increasing content of zwitterionic groups, the intensity of the peak decreases, implying that the ordered structure in PU chains is reduced. This is reasonable because the incorporation of zwitterionic groups might weaken the hydrogen bonds interaction between the soft and hard segments that is beneficial to the ordered arrangement.[27]

3.3 AFM analysis

Fig. 3 shows the AFM phase images of PU-0, iNPU-12 and iNPU-30 coating films. All of them show more or less micro-phase separated surface morphologies. It has been reported that polyurethanes prepared from different chain extenders exhibit diverse morphological structure, and many factors such as surface elasticity and adhesion force are all related to the AFM topographic images.[28] Here according to the occupied area and interface energy,[29] the bright regions are attributed to the aggregation of hard segments in the PU chains and the dark background is owing to soft segments. Clearly, more aggregation of hard segments and micro-phase separation can be observed in iNPU coatings with higher contents of zwitterionic groups. As discussed in FT-IR section, the incorporation of higher M_w of $DMA(OH)_2$ as chain extender into iNPU-30 and its further ionization bring about not only higher hard-segment contents than that in PU-0, but also stronger interactions within the region accordingly, which consequently results in the increased micro-phase separation.

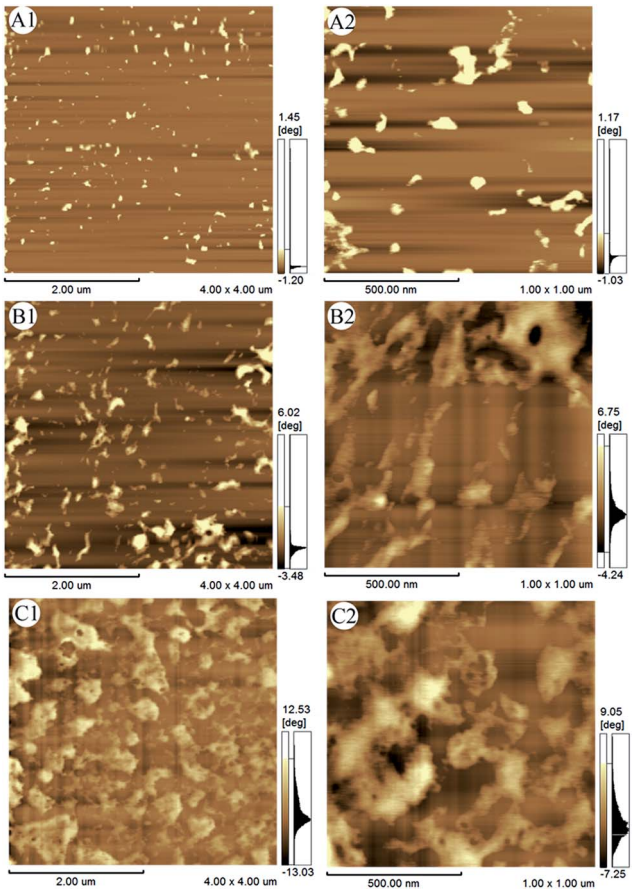

Fig. 3 AFM phase images of polyurethane coatings with different contents of zwitterionic groups: PU-0 (A1, A2), iNPU-12 (B1, B2), and iNPU-30 (C1, C2); observation range: 4 μm × 4 μm (A1, B1 and C1) and 1 μm × 1 μm (A2, B2 and C2).

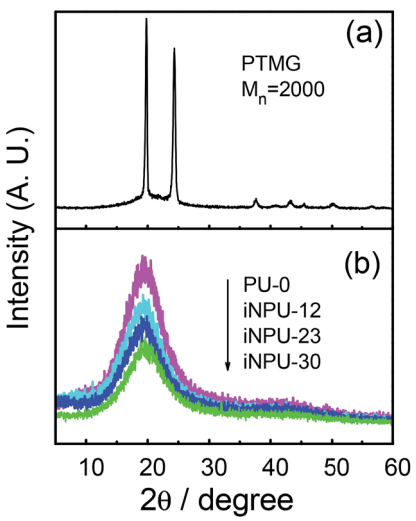

Fig. 2 (a) XRD pattern of PTMG and (b) synthesized polyurethane films with different content of zwitterionic groups.

3.4 Mechanical property measurement

The mechanical property of polyurethane coating films have been measured by tensile testing as shown in Fig. 4. It can be seen that all the samples show an elastic behaviour initially, *i.e.*, the stress increases with the strain, then reached to the yield point. Subsequently, the polyurethane films deform plastically before fracture.[30] In comparison, the PU-0 experiences a localized yielding before fracture (so called ductile failure), whereas the iNPU films exhibit a feature of necking and cold drawing behaviour. Namely, the stress keeps a constant force at which the elongation of the films are further increased and can be several times than the original length (so called stable necking,

Open Access Article. Published on 23 May 2017. Downloaded on 2/10/2026 8:12:29 PM.
This article is licensed under a Creative Commons Attribution 3.0 Unported Licence.

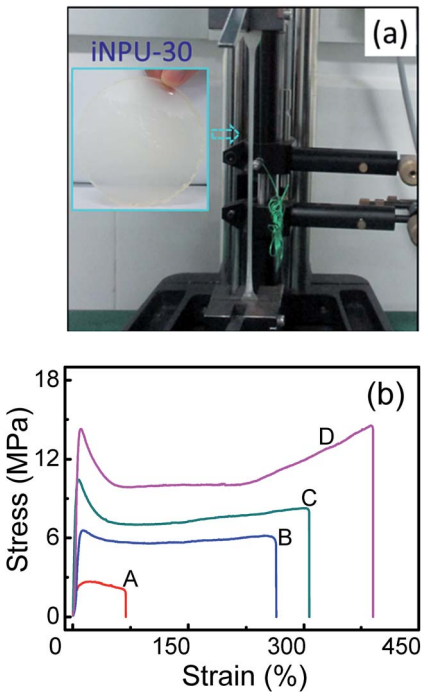

Fig. 4 Tensile testing: (a) experimental photograph of iNPU-30, and (b) stress–strain curves of synthesized polyurethane with different contents of zwitterionic groups: (A) PU-0, (B) iNPU-12, (C) iNPU-23 and (D) iNPU-30.

as shown in Fig. 4a).[30] As the stretching continues, the stress increases again until breaking. For iNPU-30, the elongation at break (EB) of 374 ± 22.6% corresponds to the tensile strength (TS) of 14.31 ± 0.26 MPa, as derived from the stress–strain curves (Fig. 4b). Such strain hardening effect is resulted from the change of molecular orientations under stretching.[31] It is obvious that the improved tensile strength and toughness of the iNPU films are positively correlated with the contents of zwitterionic groups. It can be related to three reasons. Firstly, the component of hard segment is increased due to the introduction of zwitterionic groups, which is conductive to better mechanical property since the hard segment serves as a pseudo physical cross link point.[32] Secondly, compared with 1,4-BD as chain extender for PU-0, the $DMA(OH)_2$ in iNPU contains more polar groups which can interact with the –NH–COO groups, resulting in enhanced intermolecular interaction force.[33] The further introduced sulfonate ($-SO_3$) groups by ionization or betainization contribute to the hydrogen bonding interaction within the hard segments. Thirdly, zwitterions can serve as organic fillers in the zwitterionic polyurethane, leading to the increased TS and EB of iNPU films.[34]

3.5 Dynamic mechanical thermal analysis (DMTA)

Due to the intrinsic thermodynamic incompatibility of soft segment and hard segment in polyurethanes, its thermal and mechanical behaviours are closely relevant to the ratio of the two segments, the density of chemical crosslinking and the degree of micro-phase separation.[35,36] DMTA technique is more sensitive to measure glass transition temperature (T_g) than DSC, and can provide information about side-chain or main-chain motions in specific regions of the polymer and local mode relaxation.[31] Fig. 5 shows the dynamic mechanical properties of PU-0 and iNPU with different contents of zwitterions. The E' characterizes the ability of the polymer to store energy or elastic behaviour, and is a measure of polymers stiffness.[37] And the E'' reveals the tendency of polymer to dissipate energy or viscous behavior, when the material is subjected to deformation.[30] It can be seen that all the polyurethane samples exhibit similar trend with increasing temperature. During the transition from glass state to elastomeric state, a quick and sharp decrease in the E' corresponding to the transition peaks in both E'' and tan delta curves are observed, thus the T_g is determined (dotted line) shown in Fig. 5.[38] That the T_g defined from E'' peak shifts from −69 °C for PU-0 to −77 °C for iNPU-30, suggests that the incorporated zwitterionic groups possibly make the soft

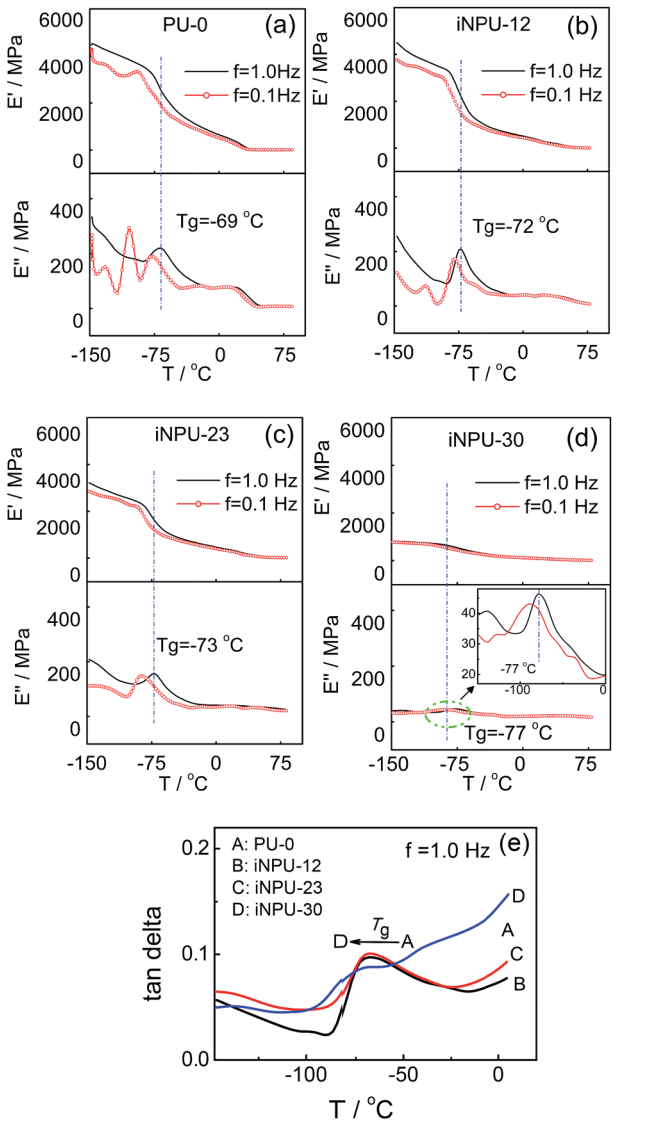

Fig. 5 Storage modulus (E'), loss modulus (E'') and tan delta of synthesized polyurethane films with different content of zwitterionic groups: (a) PU-0; (b) iNPU-12; (c) iNPU-23; (d) iNPU-30; (e) tan delta.

This journal is © The Royal Society of Chemistry 2017

Open Access Article. Published on 23 May 2017. Downloaded on 2/10/2026 8:12:29 PM.
This article is licensed under a Creative Commons Attribution 3.0 Unported Licence.

segments of polyurethane more flexible due to the reduced interaction between the soft and hard segments and the enhanced micro-phase separation of the iNPUs. In addition, E' and E'' values decrease progressively from PU-0 to iNPU-30 compared at the same temperature, indicating that the deformability of the polyurethane films increases accordingly. Obviously, the iNPU-30 film is the most flexible. The features of lower T_g and better flexibility make the iNPU favorable for leather coatings with fine weatherability.

Fig. 5e also shows that the T_g obtained from tan delta is slightly higher than those from E'' peak or E' drop, because tan delta peak not only responds to the volume fraction of the relaxation phase during glass transition process, but also it is connected with the amorphous phase.[39] It is noted that for all the polyurethanes, several small peaks appear at the temperatures lower than T_g in the E'' curves as well as decreasing steps in E' at $f = 0.1$ Hz, which are mainly associated with the secondary transitions named as β, γ and δ transition due to the rotations of terminal groups or side chains, or crankshaft motion of some segments of the main chain.[38]

3.6 Wettability property analysis

The hydrophilicity of substrate surface, characterized by water contact angle (WCA), is related to its antifouling ability because it profoundly influences the ability to resist protein adsorption.[40] And protein-resistant coatings may also resist microbial attachment, colonization and subsequent biofilm formation. Fig. 6 reveals that the incorporated zwitterionic groups make the surface of iNPU films more hydrophilic due to the increased interaction energy between the interface and water.[40] The more zwitterionic groups are introduced, the lower WCA and the better hydrophilicity the iNPU surfaces have, which is consistent with previous reports.[41] The improved wetting property is benefit to the anti-biofouling of the iNPU coating materials.

3.7 Anti-microbe adhesion property

In our previous study, the zwitterionic polyurethane shows effective nonspecific protein resistance.[15] Such polyurethanes with protein resistant property may also exhibit antimicrobial and anti-biofouling performances.[42] Although the zwitterion based polymer surfaces exhibit improved antibacterial adhesion ability in underwater applications observed by confocal laser scanning microscope, SEM or fluorescence microscopy,[43] the antimicrobial adhesion performance of the iNPU coatings against airborne spores has not been reported. Here, we tested it on macroscopic materials leather by using *A. niger* as culture strain due to its obvious colour change during growth and propagation process (shown in Fig. 7). After incubation for seven days, the black colonies of *A. niger* first appears on the uncoated leather surface. With the time extending, more and more molds are adsorbed and propagated on the uncoated sample and the leather coated with PU-0. Whereas, the iNPU coatings with higher contents of zwitterions show less adsorption of *A. niger*, exhibiting reasonably good anti-mold performance. The mechanism can be assumed that the zwitterions in iNPU can absorb the water molecules in the air due to the strong hydration capacity of zwitterionic groups with a balanced charge and further form hydrated layer, which thus can prevent microbial adhesion.

3.8 Anti-antibacterial property

The antibacterial properties of PU-0 and iNPU coating films are further evaluated by agar diffusion method, and the results are shown in Fig. 8. There are no obvious inhibition zones observed for all the samples after 48 h incubation. It means that the iNPU do not exhibit apparent contact-killing antibacterial property against *E. coli* and *S. aureus*. The reason could be that the zwitterionic polyurethanes are not bactericidal,[13] although it has antimicrobial adhesion effect. With regard to leather antifouling coatings, risks and restrictions on the use of biocide-releasing coatings have made the generation of nontoxic antifouling surfaces more important. Therefore, the iNPU can be used as antimicrobial adhesive coating, interfering with the microbe to attach to leather, textiles, marine and surgical equipment, *etc.* In addition, the polyurethane films getting white and non-

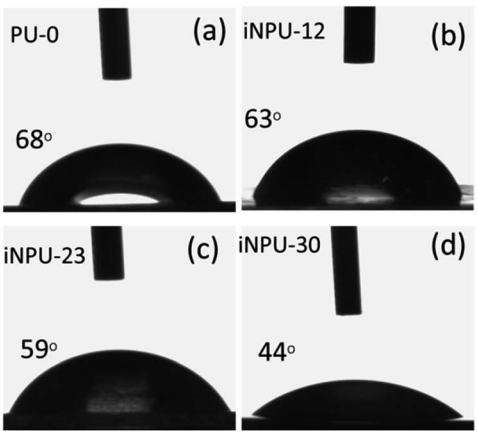

Fig. 6 Static contact angle (SCA) of synthesized polyurethane films with different content of zwitterionic groups: (A) PU-0, (B) iNPU-12, (C) iNPU-23, and (D) iNPU-30.

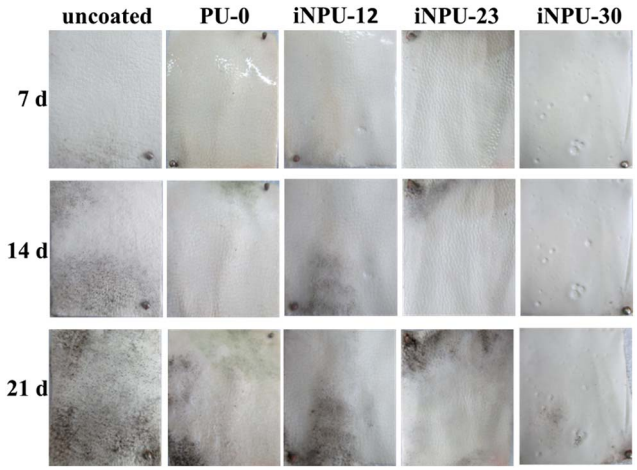

Fig. 7 Anti-mold adhesion property of leather samples coated with the synthesized polyurethane with different contents of zwitterions.

Open Access Article. Published on 23 May 2017. Downloaded on 2/10/2026 8:12:29 PM.
This article is licensed under a Creative Commons Attribution 3.0 Unported Licence.

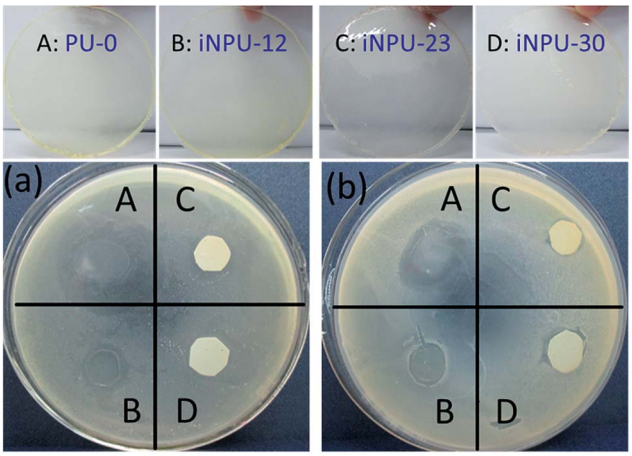

Fig. 8 Antibacterial properties of the synthesized polyurethane coatings with different content of zwitterions against: (a) Gram-positive bacterium *E. coli* and (b) Gram-negative bacterium *S. aureus*.

transparent with the increasing content of zwitterions, due to the strong hydration of the zwitterionic groups with the surrounding water. The edge of PU-0 film was partly damaged by moisture and the bacteria owing to its weak strength and toughness.

4 Conclusions

The studies on the effect of zwitterionic groups on the microstructure and performance of zwitterionic polyurethane (iNPU) coatings can lead to the following conclusions. The incorporation of zwitterionic groups into hard segment of polyurethane can create more hydrogen bonding and polar interactions within this region, and thus makes the hard components more thermodynamically incompatible with soft segment. As the content of zwitterionic group increases, the ordered structure in PU chains is reduced, and the micro-phase separation degree is increased. Furthermore, the tensile property of the iNPU coating films is significantly improved with the increase of zwitterionic groups; meanwhile, the T_g of the films decrease and the deformability increases accordingly. The presence of zwitterionic group results in the improved wetting property of polyurethane coatings. As such, the iNPU coatings with high zwitterionic group contents exhibit reasonably good anti-mold adhesion performance, although without contact-killing antibacterial ability. The synthesized zwitterionic polyurethanes can be potentially used as antimicrobial adhesive coating materials.

Acknowledgements

The financial support of National Natural Science Foundation (NNSF) of China (21476148, 21276166, 51673074) and Innovation Team Program of Science & Technology Department of Sichuan Province (2017TD0010) is gratefully acknowledged.

Notes and references

1 C. Dong, Z. Wang, J. Wu, Y. Wang, J. Wang and S. Wang, *Desalination*, 2017, **401**, 32–41.
2 V. C. Thompson, P. J. Adamson, J. Dilag, D. B. U. Uswatte, K. Blok, A. Srikantharajah and I. Köper, *RSC Adv.*, 2016, **6**(58), 53303–53309.
3 S. Palanichamy and G. Subramanian, *Prog. Org. Coat.*, 2017, **103**, 33–39.
4 S. Natarajan, M. Bhuvaneshwari, D. S. Lakshmi, P. Mrudula, N. Chandrasekaran and A. Mukherjee, *Environ. Sci. Pollut. Res.*, 2016, **23**(19), 19529–19540.
5 S. Chen, L. Yuan, Q. Li, J. Li, X. Zhu, Y. Jiang and F. J. Stadler, *Small*, 2016, **12**(26), 3516–3521.
6 G. Liu, K. Li, Q. Luo, H. Wang and Z. Zhang, *J. Colloid Interface Sci.*, 2017, **490**, 642–651.
7 P. Król, *Prog. Polym. Sci.*, 2007, **52**(6), 915–1015.
8 C. S. Gudipati, J. A. Finlay, J. A. Callow, M. E. Callow and K. L. Wooley, *Langmuir*, 2005, **21**(7), 3044–3053.
9 N. Punitha, P. Saravanan, R. Mohan and P. S. Ramesh, *Appl. Surf. Sci.*, 2016, **392**, 126–134.
10 J. Cao, N. Chen, Y. Chen and X. Luo, *Int. J. Mol. Sci.*, 2010, **11**(4), 18701–18877.
11 P. N. Coneski and J. H. Wynne, *ACS Appl. Mater. Interfaces*, 2012, **4**(9), 4465–4469.
12 J. Huang and W. Xu, *Appl. Surf. Sci.*, 2010, **256**(12), 3921–3927.
13 I. Banerjee, R. C. Pangule and R. S. Kane, *Adv. Mater.*, 2011, **23**(6), 690–718.
14 C. Ma, H. Zhou, B. Wu and G. Zhang, *ACS Appl. Mater. Interfaces*, 2011, **3**(2), 455–461.
15 C. Wang, C. Ma, C. Mu and W. Lin, *Langmuir*, 2014, **30**(43), 12860–12867.
16 B. Ahmadi, M. Kassiriha, K. Khodabakhshi and E. R. Mafi, *Prog. Org. Coat.*, 2007, **60**(2), 99–104.
17 ASTM, *Standard Test Method for Tensile Properties of Thin Plastic Sheeting*, Philadelphia, PA, 1998.
18 A. J. DeCross, B. J. Marshall and R. W. Mccallum, *J. Clin. Microbiol.*, 1993, **8**, 1971–1974.
19 C. M. Brunette, S. L. Hsu and W. J. Macknight, *Macromolecules*, 1982, **15**(1), 71–77.
20 H. S Lee, Y. K. Wang, W. J. MacKnight and S. L. Hsu, *Macromolecules*, 1988, **21**(1), 270–273.
21 S. K. Pollack, D. Y. Shen, S. L. Hsu, Q. Wang and H. D. Stidham, *Macromolecules*, 1989, **22**(2), 551–557.
22 C. B. Wang and S. L. Cooper, *Macromolecules*, 1983, **16**(5), 775–786.
23 M. F. Sonnenschein, *Polyurethanes: Science, Technology, Markets, and Trends*, John Wiley & Sons, 2015, ch. 3, pp. 105–126.
24 M. Sadeghi, M. A. Semsarzadeh, M. Barikani and B. Ghalei, *J. Membr. Sci.*, 2010, **354**(1), 40–47.
25 J. Hu and S. Mondal, *Polym. Int.*, 2005, **54**(5), 764–771.
26 W. F. Billmeyer, *Textbook of Polymer Science*, John Wiley & Sons, 2000, ch. 14, pp. 238–290.
27 L. Wang, Y. Shen, X. Lai and M. Liu, *J. Polym. Res.*, 2011, **18**(3), 469–476.
28 A. Wolińska-Grabczyk, J. Żak, J. Muszyński and A. Jankowski, *J. Macromol. Sci., Part A: Pure Appl.Chem.*, 2003, **40**(3), 225–237.

 This journal is © The Royal Society of Chemistry 2017

Open Access Article. Published on 23 May 2017. Downloaded on 2/10/2026 8:12:29 PM.
This article is licensed under a Creative Commons Attribution 3.0 Unported Licence.

29 C. Ma, Y. Hou, S. Liu and G. Zhang, *Langmuir*, 2009, **25**(16), 9467–9472.
30 I. M. Ward and J. Sweeney, *Mechanical properties of solid polymers*, John Wiley & Sons, 2012, ch. 3, pp. 31–59.
31 D. Bower, *An Introduction to Polymer Physics*, Cambridge University Press, 2002, ch. 6, pp. 162–185.
32 D. K. Chattopadhyay, B. Sreedhar and K. V. S. N. Raju, *Ind. Eng. Chem. Res.*, 2005, **44**, 1772–1779.
33 S. Nayak, H. Verma and T. Kannan, *Colloid Polym. Sci.*, 2010, **288**, 181–188.
34 S. F. Mo, Y. Yang, F. J. Stadler, S. Chen and H. Yang, *J. Mater. Chem. A*, 2015, **3**, 2924–2933.
35 J. L. Vilas, J. M. Laza, C. Rodriguez, M. Rodriguez and M. L. Leon, *Polym. Eng. Sci.*, 2015, **53**, 744–751.
36 H. J. Qi and M. C. Boyce, *Mech. Mater.*, 2005, **37**, 817–839.
37 M. Neag, *ASTM Manual*, American Society for Testing and Materials (ASTM) Philadelphia, PA, 1995, pp. 841–864.
38 D. Macocinschi, D. Filip, S. Vlad, M. Cristea and M. Butnaru, *J. Mater. Sci.: Mater. Med.*, 2009, **20**, 1659–1668.
39 E. A. Turi, *Thermal characterization of polymeric materials*, Academic Press, 1981, ch. 6, pp. 595–704.
40 Q. Li, Q. Y. Bi, B. Zhou and X. L. Wang, *Appl. Surf. Sci.*, 2012, **258**, 4707–4717.
41 X. Yi, S. S. Li, J. Xin, X. Tao, W. Rui and C. S. Zhao, *J. Colloid Interface Sci.*, 2014, **443**, 36–44.
42 F. Mo, H. Ren, S. Chen and Z. Ge, *Mater. Lett.*, 2015, **145**, 174–176.
43 J. Ma, C. Ma and G. Zhang, *Langmuir*, 2015, **31**, 6471–6478.